

# Virtual Multisensor Assistance System: The Virtual Measurement Components

Klaus Haskamp

Institute of Measurement and Automatic Control, Leibniz Universität Hannover

Nienburger Str. 17, 30167 Hannover, Germany

email: klaus.haskamp@imr.uni-hannover.de

## Abstract

Virtual measurement systems are applied for systematic analysis of the measurement process. The estimation of the influence of the system parameters with respect to the reachable measurement uncertainty and the optimal measurement setup, concerning different optimization criteria like holistic or fast measurements, are the main fields of application of virtual measurement systems. The setup of a virtual multisensor assistance system for the design of measurement procedures is the main task of the subproject B5 of the CRC 489. The assistance system is build from a fringe projection sensor, a shadow projection sensor and several rotational and linear axes. The numerical simulation of the different systems and the adjustment of the virtual and the real systems are one of the core components of the research. Another task is to decide, which measurement system should be used for the measurement concerning the minimum measurement uncertainty. In this paper the virtual systems of the used measurement systems and the theoretical background should be shortly discussed.

## Keywords:

Virtual measurement, shadow projection, fringe projection, measurement uncertainty

## 1 INTRODUCTION

The quality management is one of the most important parts of the production process. The quality management must ensure that the significant geometric parts can be measured with measurement uncertainties which are less than pre-defined tolerances. To verify a high accuracy a measurement uncertainty analysis have to be accomplished with an appropriate reference workpiece. The result of the analysis is an estimation of the reachable accuracy of the geometric areas respectively the remaining measurement uncertainty. The effort of time and money, which is combined with the analysis, can be reduced using a numerical simulation of the measurement systems [13]. Using the virtual measurement system the whole measurement process can be simulated [9, 13]. In combination with Monte-Carlo methods it is possible to estimate measurement uncertainties from a CAD-model. For the realization the virtual measurement system and the virtual measurement process have to be implemented in the computer. The scheme of the virtual measurement is shown in figure 1. The virtual workpieces, described using polygons, are measured by the virtual measurement systems. After the measurement a measurement uncertainty analysis and an inspection of the measurability of the workpiece is done.

In addition of the use of the virtual system as a tool for the estimation of uncertainties the virtual system can be integrated in an assistance system. The main task of the assistance system is the calculation of optimal and component geometry adapted measurement strategies concerning different criteria [13]. The criteria can be a

time minimum

hollistic

measurement uncertainty

measurement. This is the main field of research of the subproject B5 „Complete Geometry Inspection“ of the collaborative research centre 489 (CRC 489) “Process chain for the production of precision-forged high-performance parts”. The used virtual assistance system is build up from a fringe projection system, a shadow projection system and several rotational and linear axes.

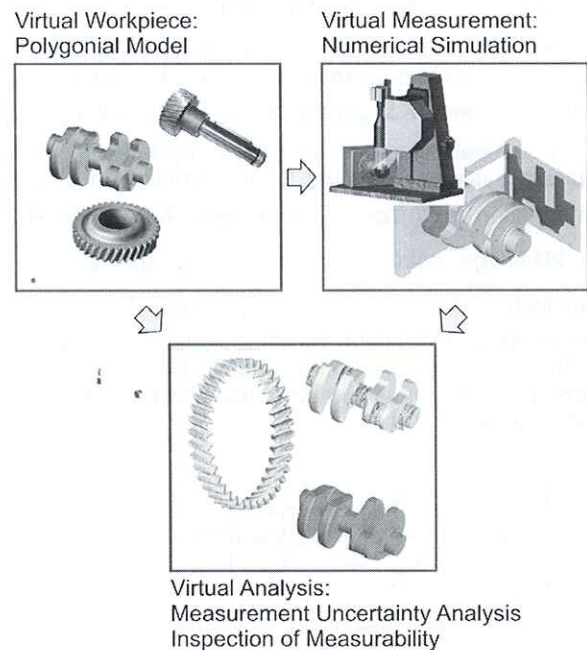


Figure 1: Virtual Measurement, © IMR

In this paper the simulation models of the virtual measurement systems and the used physical theory will be shortly discussed.

## 2 FRINGE PROJECTION SYSTEM

The basic components of a fringe projection system are one or more projectors and one or more cameras. The illumination unit sends out coded light onto the objects surface and the camera records the deformed light [12]. The basic principle of the coding of the light is that a relationship between the camera pixel  $\{i, j\}$  and the projector phase  $\phi$  can be found. This information is used to reconstruct the object surface with the triangulation principle.

The model of the fringe projection system is based on the fundamentals of geometric optics [4, 10]. The geometric setup and the position and orientation of the coordinate systems, which are necessary for the formulation of the

linear transformations, are shown in figure 2. The used fringe projection system is build up of one projector and one camera. The camera has an object-sided telecentric, which is considered in the simulation. Following the transformation from the object coordinate system to the camera/projector pixels should be explained in detail.

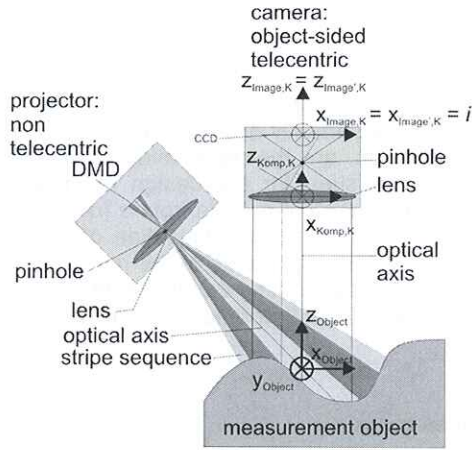


Figure 2: Model of the Fringe Projection System, © IMR

The postpositioned indices "C" and "P" denote the affiliation to the **C**amera respectively the **P**rojector. The coordinate system  $KS_{Obj}$  is the object coordinate system and the inertial reference coordinate system [1]. The coordinate systems are used for the formulation of the transformation from the 3D-coordinates  $\mathbf{X} = [x, y, z, 1]^T$  to a 2D-image point from the camera  $\boldsymbol{\eta}_c = [i, j, 1]^T$  respectively the projector  $\boldsymbol{\eta}_p = [\phi, \psi, 1]^T$ . The transformation sequence is shown in figure 3. Due to the fact that a projector can be treated like an inverse camera the transformations are explained exemplarily with the camera [12].

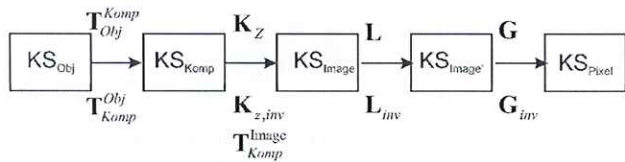


Figure 3: Transformation Steps

The first step is the homogenous transformation from the object coordinate system to the component coordinate system  $KS_{Komp,K}$ , using the matrix  $\mathbf{T}_{Obj}^{Komp}$ , [6]:

$$\mathbf{T}_{Obj}^{Komp} = \begin{bmatrix} \mathbf{R}_{Obj}^{Komp} & \mathbf{r}_{Obj} \\ \mathbf{0}^T & 1 \end{bmatrix}$$

with  $\mathbf{R}_{Obj}^{Komp}$  as the rotational part and  $\mathbf{r}_{Obj}$  as the translatorial part.

Following the points are transformed into the image coordinate system  $KS_{Image,K}$  using a telecentric projection  $\mathbf{K}_Z$ , [5]:

$$\mathbf{K}_Z = \begin{bmatrix} 1 & 0 & 0 & 0 \\ 0 & 1 & 0 & 0 \\ 0 & 0 & 0 & 1 \end{bmatrix}$$

The nonlinear distortion errors can be expressed with the distortion function  $\mathbf{L}$ , [2, 7]:

$$\mathbf{X}_{Image'} = \mathbf{L}(\mathbf{X}_{Image}, \mathbf{k})$$

with  $\mathbf{k}$  as the parameter vector. The distortion can be subdivided into three different distortion types [2, 7]:

$$\text{radial symmetric } \delta \mathbf{x}_r = [\delta x_r \quad \delta y_r]^T$$

$$\text{radial asymmetric } \delta \mathbf{x}_d = [\delta x_d \quad \delta y_d]^T$$

$$\text{affinity and shear } \delta \mathbf{x}_a = [\delta x_a \quad \delta y_a]^T$$

The last step is the transformation into the pixel coordinate system  $KS_{Pixel,K}$  with the matrix  $\mathbf{G}$  and a discretization into discrete integer numbers (pixels):

$$\mathbf{G} = \begin{bmatrix} 0 & 1 & \frac{h_{CCD}}{2} \\ 1 & 0 & \frac{b_{CCD}}{2} \\ 0 & 0 & 1 \end{bmatrix},$$

whereas  $b_{CCD}$  and  $h_{CCD}$  are the dimensions of the pixel plane of the camera chip.

The transformations for the projector are the same for the camera. The model parameters were identified through a calibration and a complete description of the virtual measurement system is available.

### 3 SHADOW PROJECTION SYSTEM

Shadow projection systems are applied for contour measurements [5]. Therefore the measurement object is lighted from one side with parallel monochromatic laser light, as shown in figure 4.

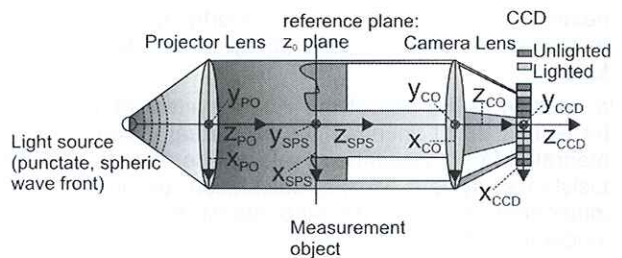


Figure 4: Model of the Shadow Projection System, © IMR

The light is interrupted from the edge of the object and the projected shade is detected from a CCD row sensor, which is equipped with a telecentric projection optic. To calculate the expansion of the projected shadow the shadow boundary have to be extracted. Therefore the gray scale values from bright and dark crossings were evaluated using sub pixel methods and interpolated using polynom functions. The shadow border can be found at the pixel-position, where the interpolated gray scale trend deceeds a pre defined digitalisation barrier.

For the simulation a reference coordinate system is needed. This coordinate system is the object coordinate system (Object), which is shown in figure 4. Furthermore a coordinate system is assigned to each optical component. Therewith it is possible to simulate misalignments concerning tilt, like the inclined orientation of the optical axes. In the simulation process it is necessary to project the virtual measurement object onto a reference plane, which is called  $z_0$ . The reference plane is the  $xy$ -plane in the shadow projection coordinate system (SPS) and the projection is central perspective and parallel with respect to the  $xy$ -plane.

The simulation of the shadow projection system is based on the foundations of the scalar diffraction theory [3]. The relevant information - the intensity of the CCD-matrix  $I_{CCD}$  - is calculated by solving the Helmholtz-Kirchhoff integral with the Rayleigh-Sommerfeld solution [12]. The integral is calculated sequentially for different planes, which are shown in figure 3. Thereby a stage is a planar surface and the electric field respectively the intensity is calculated for discrete points, which should be expressed by the postpositionend indices " $_{xy}$ ".

$$U_{xy}(P_0) = \frac{1}{j\lambda} \Sigma \Sigma A \exp(j\phi)$$

$$A = U_{xy}(P_1) \cdot \frac{\cos(\mathbf{n}, \mathbf{r}_{01}) \delta x \delta y}{|\mathbf{r}_{01}|}$$

$$\phi = k |\mathbf{r}_{01}|$$

with  $U_{xy}(P_0)$  as the electric field at the observation point  $P_0$ ,  $U_{xy}(P_1)$  as the electric field at the point  $P_1$  of the aperture,  $k$  as the wave number,  $\mathbf{n}$  as the normal vector of the aperture pointing outwards and  $\mathbf{r}_{01}$  as the length from point  $P_0$  to  $P_1$ . The sequential calculation of the CCD-matrix intensity starts with the computation of the electric field  $E_{PO,xy}$  respectively the intensity

$I_{PO,xy}$  at the projector lens plane. The light propagation is described using a punctate light source and the optical concept of the gauss beam [3].

The Rayleigh-Sommerfeld formulation needs two dimensional apertures. In our case we have a measurement object with a three dimensional shape. The two dimensional aperture is created by the parallel projection of the three dimensional object onto the reference plane. Following the electric field  $E_{z_0,xy}$  is computed for each point which is part of the projected surface using the Rayleigh-Sommerfeld solution. The next stage is the aperture of the camera lens. This means that the electric field  $E_{CO,xy}$  for the camera lens plane has to be calculated. The last stage is build from the CCD-Matrix, so that  $E_{CCD,xy}$  respectively  $I_{CCD,xy}$  have to be computed.

The components are not optimal and accurate. The optical errors have to be considered and modelled in the numerical simulation. In this simulation the errors were expressed as phase errors  $\Delta\phi$  of the wave fronts and were considered as an additionally phase term in the diffraction integral. The spherical waves, which starts from

the projector and the camera lens, get a phase error.  $\Delta\phi$  depends on the position on the aperture and is mathematically described using Zernike polynom functions [11]:

with

$$Z_n^m(\rho, \phi) = R_n^m(\rho) \cos(m\phi) = \Delta\phi$$

$$R_n^m = \sum_{k=0}^{\frac{n-m}{2}} \frac{(-1)^k (n-k)! \rho^{n-2k}}{k! \left( \left( \frac{n+m}{2} \right) - k \right)! \left( \left( \frac{n-m}{2} \right) - k \right)!}$$

$\rho$  is the normalized radial distance and  $\phi$  the azimuthally angle. For example the equation for astigmatism or coma is [13]:

$$Z_{Astig} = \rho^2 \sin(2\phi)$$

$$Z_{Coma} = (3\rho^3 - 2\rho) \sin(\phi)$$

Using Zernike polynoms the diffraction integral is formulated in the following way:

$$U_{xy}(P_0) = \frac{1}{j\lambda} \Sigma \Sigma A \exp(j\phi(x, y))$$

$$A = U_{xy}(P_1) \cdot \frac{\cos(\mathbf{n}, \mathbf{r}_{01}) \delta x \delta y}{|\mathbf{r}_{01}|}$$

$$\phi(x, y) = k |\mathbf{r}_{01}| + \Delta\phi$$

The algorithms have been implemented in C++ using the CUDA programming technique to minimize the simulation time. The calculations were executed on the graphic card (GPU). The main advantage is that the calculations can be parallelized and therewith the simulation time be reduced with approximately the factor 100.

#### 4 CONCLUSION AND OUTLOOK

In this work the virtual measurement systems of a fringe projection system and a shadow projection system were presented. Beside the geometric model the used theoretical foundations have been described.

The virtual measurement systems can be combined with their virtual measurement processes to a virtual multisensor assistance. The assistance system can be used parallel to design phase for the inspection of the measurability of work pieces. Furthermore the system can be used for an estimation if the pre-defined tolerances are measurable with an appropriate accuracy.

#### 5 ACKNOWLEDGEMENT

The authors would like to thank the German Research Foundation (DFG) for funding the project B5 "Geometric Analysis" within the Collaborative Research Center (CRC) 489 "Process Chain for the Production of Precision Forged High Performance Components".

#### 6 REFERENCES

- [1] Böttner, T.: Messunsicherheitsbetrachtungen an einem virtuellen Streifenprojektinssystem, Dissertation, Leibniz Universität Hannover, 2009

- [2] Brown, D.C.: Close-range camera calibration, in Photogrammetrie Engineering, pp. 855 – 866, 1971
- [3] Goodman, J.W.: Fourier Optics, Roberts and Company Publishers, Third Edition, 2005
- [4] Hartley, R.I.; Zissermann, A.: Multiple View Geometry in Computer Vision, Cambridge University Press, 2. Auflage, 2004
- [5] Kästner, M.: Optische Geometrieprüfung präzisionsgeschmiedeter Hochleistungsbauteile, Dissertation Universität Hannover, 2008
- [6] Luhmann, T.: Nahbereichsphotogrammetrie, Wichmann Verlag, 2000
- [7] Remondino, F.; Fraser, C.S.: Digital Camera Calibration Methods: Considerations & Comparisons, ISPRS Commission V Symposium Image Engineering and Vision Metrology, 2006
- [8] Schmitt, R.; Koerfer, F.; Bichmann, S.: Modellierung optischer Messprozesse, Technisches Messen TM, pp. 230 - 236, 2008
- [9] Schmitt, R.; Koerfer, F.; Sawodny, O.; Zimmermann, J.; Kürger-Sehm, R.; Xu, M.; Dziomba, T.; Koenders, L.; Goch, G.; Tausendfreund, A.; Patzelt, S.; Simon, S.; Rockstroh, L.; Bellon, C.; Staude, A.; Woias, P.; Goldschmidtbing, M.; Rabold, M.: Virtuelle Messgeräte, Technisches Messen TM, pp. 298 - 310, 2008
- [10] Schreer, O.: Stereosynthese und Bildanalyse, Springer Verlag Berlin, Heidelberg, 2005
- [11] Singer, W.; Totzeck, M.; Gross, H.: Handbook of Optical Systems, edited by Herbert Gross, Wiley-VCH Verlag GmbH & Co. KGaA, Volume 2, 2005
- [12] Valkenburg, R.J.; Mc Ivor, A.M.: Accurate 3D Measurement using a structured light system, in Image and Vision Computing, pp. 99 – 110, 1998
- [13] Weckenmann, A.; Hartmann, W.; Weickmann, J.: Model and simulation of fringe projection measurements as part of an assistance system for multi-component fringe projection sensors, In: Duparré, A.; Geyl, R. (Hrsg.): Proceedings of SPIE Vol. 7102, 2008